

## Heat Capacity of BN and GaN binary semiconductor under high Pressure-Temperature (PT) from First-principles

B. P. Pandey<sup>1</sup>, V. Kumar<sup>2</sup>

<sup>1</sup>(ECE, GLA University (Mathura) India-281406)

<sup>2</sup>(Electronics Engineering, Indian School of Mines, (Dhanbad) India-826004)

---

**Abstract:** In this paper, we have calculated the molar heat capacity for cubic zinc blende (cZB) BN and GaN binary semiconductors at high pressure-temperature (PT). For the calculation of heat capacity, we firstly obtained the Debye temperature ( $\Theta_D$ ) variation with temperature and at higher temperature it becomes constant with temperature in quasi-harmonic approximation limits. We have also calculated the static Debye temperature ( $\Theta_D$ ) from elastic constant for the both BN and GaN binary semiconductors. The elastic constants are calculated from the energy-strain relation using plane wave method in DFT approach. All the calculated results are well consistence with experimental and reported data.

**Keywords:** Debye temperature, DFT, LDA, PDOS, QHA, USPP etc.

---

### I. INTRODUCTION

The III-V group of nitrides have attracted due to their potential applications in the fields of optoelectronic such as wide band gap, light sources, super hardness properties, uses at high temperature and pressure, high density data storage capacity and high power conversion efficiency[1-2]. The hardest natural materials we have ever known as diamond. Cubic boron nitride (cBN) is a second promising hardest material that contains many important physical and chemical properties in high temperature-pressure range after diamond. cBN has been utilized in many industrial applications as cutting tools and abrasives[3]. The binary compound cBN and cGaN crystallizes in a zinc blend structure which closely resembles that of diamond, each atom being tetragonally linked to four neighboring boron or nitrogen atoms by strong covalent bonds. Charge accumulates strongly between the atoms due to the strong interatomic interaction of s and p orbital's. Moreover, because of its wide band gap and good thermal conductivity, cBN and cGaN also has the potential application for the high-temperature, high-power electronic applications and utilized from visible spectrum to the ultraviolet spectrum by varying its wide bandgap[4-5]. These two are also very prominent binary compounds for extreme condition as high pressure-temperature. Therefore, experimental and theoretical investigations are of a great interest to physicists and researchers community. Earlier work [6-8] explored more information with improved accuracy about the characteristics of cBN and cGaN. It was found that cBN and cGaN were thermodynamically stable at ambient environment but still the structural phase and its thermodynamic stability of cBN and cGaN under high temperature -pressure remain uncertain.

In the present work, we investigate the heat capacity at high PT of cBN and cGaN by using a first-principles plane wave method in the frame of quasi-harmonic approximation with local density approximation (LDA). We have also calculated the elastic constants from which other thermal and mechanical properties like Debye temperature ( $\Theta_D$ ) and bulk modulus ( $B_0$ ) have been calculated. We have also proposed a mathematical model for calculation of heat capacity approximating that Debye temperature is varying with temperature. The results obtained are in good agreement with the available experimental results and other reported theoretical methods.

### II. COMPUTATIONAL METHODS

First principles total energy calculations were performed using quantum-esspresso code [9]. The interaction between ions and valence electrons were described by the USPP method [10] for the both binary semiconductor. The exchange and correlation effects were treated by the local density approximation of Perdew and Zunger[11]. The k mesh was sampled according to a Monkhorst-Pack scheme as 4 4 4 with a spacing of 0.5 / Å [12].The electronic configurations for B, Ga and N are [He]2s<sup>2</sup>2p<sup>1</sup>, [Ar]3d<sup>10</sup>4s<sup>2</sup>4p<sup>1</sup> and [He]2s<sup>2</sup>2p<sup>3</sup> respectively. The valence electrons are taken as 3, 13 and 5 respectively for B, Ga and N. The 3d<sup>10</sup> electrons have taken in valence because to see the non localized effect of d shell in Ga atom. The energy cutoff in the plane wave expansion was 65Ry and cutoff for charge density was 720 Ry for the both cBN and cGaN. Convergence of relative energies with respect to the k mesh and energy cutoff was found to be better than 1 meV/atom. The cutoff of plane wave expansion is taken as high due to hard pseudo-potential of N atom. The equation of states (EOS) is used to determine equilibrium lattice parameter for cBN and cGaN. Debye

temperature and heat capacity at equilibrium lattice parameter have calculated in the frame of quasi-harmonic approximation (QHA) by fitting the thermal EOS.

### III. RESULTS AND DISCUSSION

#### 3.1 Structural properties

To calculate the structural properties we take the local density approximation (LDA) pseudo-potential for the cBN and cGaN in zinc-blend structure. The graph between total energy verses lattice parameter are plotted for cBN and cGaN in Figure 1. The calculated equilibrium lattice parameters are 3.582Å and 4.467Å for cBN and cGaN respectively from Figure 1. The calculated equilibrium lattice parameters are underestimated due to inherent property of LDA. The obtained equilibrium lattice parameter results are compared with available experimental and reported data given in Table 1. The lattice parameter in terms of volume verses pressure is calculated for two different ambient temperatures 0K and 1500K for cBN and cGaN shown in Figure 2. Figure 2 is showing that at higher pressure volumes are very less deviates from each other regardless of any temperatures range for the case of cBN but shows much deviation for cGaN as the pressure increased also the temperature will play a major role in variation of volumes verses temperature. The general behavior of volume verses pressure is decreasing in nature as pressure increased also shown in Figure 2. We have also calculated the volume variations with respect to wide temperature range at two different extreme pressures (0GPa, 150GPa) for cBN and (0GPa, 50GPa) for cGaN. From the obtained results, it is observed that volume varies with respect to temperature significantly at low pressure but very less varying at higher pressure which is true for both cBN and cGaN. The simulated results have been shown in Figure 3.

#### 3.2 Debye temperature ( $\Theta_D$ ) calculation using Elastic constants

The Debye temperature can be calculated using Elastic constants [13] whereas elastic constants are calculated at equilibrium (P=0, T=0) lattice parameter for cBN and cGaN. The stiffness constants are defined as

$$C_{ij} \equiv c_{\alpha\beta\gamma\delta} = \frac{1}{V_0} \frac{\partial^2 E_{total}}{\partial \epsilon_{\alpha\beta} \partial \epsilon_{\gamma\delta}} \quad (1)$$

where  $U = E_{total}/V_0$  is the total energy per unit volume.  $\sigma_{\alpha\beta}$  and  $\epsilon_{\alpha\beta}$  ( $\alpha, \beta = x, y, z$ ) are the components of the stress and strain tensors respectively. Due to the symmetry of cubic crystals, the stiffness constants using Voigt indices are  $C_{11}$ ,  $C_{12}$  and  $C_{44}$  [14]. For the calculation of the stiffness constant, we used the periodic DFT method to calculate the energies of cBN and cGaN crystals for the applied strain. We applied three independent strains 0,  $\pm 0.015$ ,  $\pm 0.010$ ,  $\pm 0.005$  and fitted the stiffness constants to the energy-strain relation  $U = \frac{1}{2} C_{11} \epsilon_{xx}^2$ ,  $U = (C_{11} + C_{12}) \epsilon_{xx}^2$  and  $U = 2C_{44} \epsilon_{yz}^2$  for the calculation of  $C_{11}$ ,  $C_{12}$  and  $C_{44}$  respectively. The Total energy  $E_{total}(\epsilon)$  were fitted to polynomial equation

$$E_{total}(\epsilon) = V_0 U(\epsilon) = A_0 + A_1 \epsilon + A_2 \epsilon^2 + A_3 \epsilon^3 \quad (2)$$

where  $A_0$ ,  $A_1$ ,  $A_2$  and  $A_3$  are the fitting parameters.  $A_1$  corrects inaccuracies in the variable cell optimization and  $A_3$  corrects for anharmonic terms [15]. The 3rd term  $A_2$  is the important for calculation of stiffness constants which is related by  $A_2/V_0$  is equal to  $C_{11}/2$  for strain  $\epsilon_{xx}$ ,  $(C_{11}+C_{12})$  for strain  $\epsilon_{xx} = \epsilon_{yy}$  and  $2C_{44}$  for strain  $\epsilon_{yz}$ . The calculated stiffness constants are given in Table 1. The obtained values of stiffness constants are in good agreement for cBN cGaN with the reported and available experimental data. The results shows overestimation of stiffness constants for cBN and cGaN from the experimental values. The Debye temperature,  $\Theta_D$ , defined as a measure of the cutoff frequency by  $\theta_D = \hbar \omega_D / k_B$ , is then proportional to the Debye sound velocity  $v_D$ :

$$\theta_D = \frac{\hbar}{k_B} \left( \frac{6\pi^2 N}{V} \right)^{1/3} v_D \quad (3)$$

And

$$v_D = k(v) \sqrt{\frac{B}{\rho}} \quad (4)$$

The bulk modulus B and Poisson ratio  $\nu$  of a polycrystalline material is estimated from the single crystal elastic constants by the Voigt–Reuss–Hill (VRH) approximation [16].

$\Theta_D$  and  $k(v)$  can be given in more usable format in terms of atomic weight M and Poisson ratio  $\nu$  as:

$$\theta_D = k(v) \frac{\hbar}{k_B} \left( \frac{6\pi^2 \rho}{M} \right)^{1/3} \sqrt{\frac{B}{\rho}} \quad (5)$$

And

$$k(v) = \left[ \frac{1}{3} \left[ \frac{1+\nu}{3(1-\nu)} \right]^{3/2} + 2 \left[ \frac{2(1+\nu)}{3(1-2\nu)} \right]^{3/2} \right]^{-1/3} \quad (6)$$

$\Theta_D$  can be further rewritten as:

$$\theta_D = k(v) \frac{\hbar}{k_B} (48\pi^5)^{1/6} \sqrt{\frac{r_0 B}{M}} \quad (7)$$

In this expression,  $r_0$  is the equilibrium Wigner–Seitz radius, which is defined by  $4\pi r_0^3/3=V/N=M/\rho$ . Where  $V$  is the equilibrium volume,  $N$  is the number of atoms per unit cell. The Debye temperature ( $\Theta_D$ ) obtained from the elastic constants using Eq. (7) are compared with the calculated value of  $\Theta_D$  in frame of quasi-harmonic approximation (QHA) at equilibrium ( $T=0$ ,  $P=0$ ) are given in Table 1 and also compared with the available experimental value which are in good agreement with some allowable error. The Debye temperatures vary between 1540 K (expanded BN) and 1740 K (compressed BN) for cBN [17] and 867 for cGaN[26]. These calculated values are deviated from the experimental values of due to error in bulk modulus which is varying from 2% to 10% from their experimental value.

### 3.3 Debye temperature ( $\Theta_D$ ) variation with temperature and heat capacity in quasi-harmonic approximation (QHA)

Quantum mechanical effects are very important in understanding the thermodynamic properties below the Debye temperature. The Debye temperature variation with respect to temperature below its melting temperature is also shown in Figure 4 at the equilibrium ( $T=0$ ,  $P=0$ ) lattice constant for cBN and cGaN in quasi-harmonic approximation. Heat capacity at constant volume  $C_V$  can be calculated directly from the phonon DOS under the harmonic approximation. Heat capacity at constant volume under the Debye approximation is expressed as

$$C_V = 9N_A k_B (T/\theta_D)^3 \int_0^{\theta_D/T} (h\nu/k_B T)^2 W(h\nu/k_B T) d\nu \quad (8)$$

where  $W(h\nu/k_B T)$  is weighting factor and again Eq.(8) can be rewritten as

$$C_V = r N_A k_B \int_0^\infty g(\nu) W(h\nu/k_B T) d\nu \quad (9)$$

where  $g(\nu)$  is phonon density of states (PDOS).

We have plotted the calculated total phonon DOS (PDOS) and each elemental phonon DOS in Figure 5 for cBN and in Figure 6 for cGaN at 0 K using the static equilibrium geometry obtained from the first principles. There some important observations from Figure 5 and Figure 6 are as follows: From Figure 5, Below  $800 \text{ cm}^{-1}$  frequency, equal contributions from atom B and atom N are observed in total phonon DOS of cBN and above  $800 \text{ cm}^{-1}$  frequency, B atom contributions is much larger compare to N atom in total phonon DOS of cBN. Two gaps are shown in Figure 6 around the frequency  $350 \text{ cm}^{-1}$  to  $530 \text{ cm}^{-1}$  and  $675 \text{ cm}^{-1}$ . Below  $350 \text{ cm}^{-1}$ , the total phonon DOS are mixed vibrations of atom Ga and atom N mainly dominated by Ga atom. Above  $530 \text{ cm}^{-1}$ , the total phonon DOS is mainly originated from the N atom vibrations and very small vibrations are originated from the Ga atom. The difference between  $C_P$  and  $C_V$  was given by a relationship  $C_P - C_V = VT\beta^2 B_0$ .  $V$ ,  $T$ ,  $\beta$  and  $B_0$  are molar volume, absolute temperature, volume thermal expansion coefficient and isothermal bulk modulus respectively. At  $T = 0 \text{ K}$ , the difference between the constant pressure heat capacity  $C_P$  and the constant volume heat capacity  $C_V$  is almost zero, but the difference increases almost linearly with the temperature  $T$ . The molar heat capacity at constant pressure is shown in Figure 7 at two extreme different pressure 0GPa and 150GPa for cBN, 0GPa and 50GPa for cGaN. As the pressure increases, the heat capacity does not deviate much from the Dulong-Petit limit. At high temperature, heat capacity will become constants due to constant value is obtained for the Debye temperature as shown in Figure 4 and if the temperature increase, the heat capacity at constant pressure  $C_P$  increases almost linearly with temperature. For higher temperatures, the anharmonic approximations of the Debye model is used here in which the anharmonic effect on  $C_V$  is suppressed, and  $C_V$  is very close to the Dulong-Petit limit to  $3R$ , where  $R$  ( $8.3144621 \text{ J/mol.K}$ ) represents the molar gas constant. It is more informative to plot the heat capacity data( $C_P$ )  $C_P/T^3$  vs. temperature as shown in Figure 8 and according to the Debye  $T^3$  model, the lattice vibration to  $C_P/T^3$  should approach constant value at lower temperature. If  $C_P/T^3$  vs. temperature deviated from constant value, it means others factors like electronics, magnetic etc have contributed in heat capacity ( $C_P$ ). It is well known that the contributions due to optical phonons do not obey the Debye  $T^3$  model. From Figure 8, it has been observed in cBN that optical phonons are less dominated compare to the cGaN in  $C_P/T^3$  vs. temperature graph at extreme pressure.

## IV. CONCLUSIONS

In summary, we have performed first-principles calculations for cBN and cGaN, including the equilibrium lattice parameters, volume variations at extreme conditions, Debye temperature variation with temperature, elastic constants, Debye temperature using elastic constant, total phonon DOS with phonon DOS of individual elements of cBN and cGaN and heat capacity. All the obtained results are well consistent with the previous experimental and reported results from others workers.

## REFERENCES

- [1] I.Vurgaftman, J. R. Meyer and L. R. Ram-Mohan, JAP 89 (2001) 5815-5875.
- [2] G. Chris, Van de Walle, Jorg Neugebauer, JAP 95 (2004) 3851-3879.
- [3] Tetsuya Tohei, Akihide Kuwabara, Fumiyasu Oba, and Isao Tanaka, Phys. Rev. B 73 (2006) 064304.
- [4] Hao Yan-Jun, Cheng Yan, Wang Yan-Ju, and Chen Xiang-Rong, Chin. Phys. Soc. 16(1) (2007).

- [5] G Will and P G Perkins, *Diamond Relat. Mater.* 10 (2001) 2010.  
 [6] E. Lopez-Aprezaa, J. Arriaga, and D. Olguin, *Rev. Mex. Fis.* 56 (3) (2010) 183–194.  
 [7] H Sachdev, R Haubner, B Lux and H Noth, *Diamond Relat. Mater.* 6 (1997) 286.  
 [8] V L Solozhenko, *J. Hard Mater.* 6 (1995) 51.  
 [9] P. Giannozzi et al., *J. Phys.:Condens. Matter* 21 (2009) 395502.  
 [10] D. Vanderbilt, *Phys. Rev. B* 41 (1990) 7892-7895.  
 [11] J. P. Perdew and A. Zunger, *Phys. Rev. B* 23 (1981) 5048.  
 [12] H. J. Monkhorst and J. D. Pack, *Phys. Rev. B* 13 (1976) 5188.  
 [13] Q. Chen and B. Sundman, *Acta mater.* 49 (2001) 947–961.  
 [14] E. Dieulesaint, D. Royer, *Elastic Waves in solids.* Wiley, chichester, 1980.  
 [15] E. Menendez-Proupin, S. Cervantes-Rodriguez, R. Osorio-Pulgar, M. Franco-Cisterna, H. Camacho-Montes, M.E. Fuentes, *JMBBM* 4 (2011) 1011-1020.  
 [16] R. Meister, and L. Peselnick, *J. Appl. Phys.*, 37 (1966) 4121.  
 [17] Won Ha Moona, Myung Sik Sonb, Ho Jung Hwanga, *Physica B* 336 (2003) 329–334.  
 [18] W. Rössler, *Group IV Elements, IV-IV and III-V Compounds*, 41A1 of Landolt Börnstein, Group III Condensed Matter, Springer-Verlag, Berlin, 2001.  
 [19] Y. S. Touloukian, R. K. Kirby, R. E. Taylor, and T. Y. R. Lee, *Thermal Expansion: Nonmetallic Solids*, Vol. 13 of Thermophysical Properties of Matter IFI-Plenum, New York, 1977.  
 [20] R. H. Wentorf, Jr., *J. Chem. Phys.* 26 (1957) 956.  
 [21] P. Rodriguez-Hernandez, M. Gonzalez-Diaz, A. Munoz, *Phys. Rev. B* 51 (1995) 14705.  
 [22] M. Grimsditch, E.S. Zouboulis, A. Polian, *J. Appl. Phys.* 76 (1994) 832.  
 [23] P.J. Gielisse, S.S. Mitra, J.N. Plendl, R.D. Griffiths, L.C. Mansur, R. Marshall, E.A. Pascoe, *Phys. Rev.* 155 (1967) 1039.  
 [24] G.A. Slack, S.F. Bartram, *J. Appl. Phys.* 46 (1975) 89.  
 [25] W. Sekkal, B. Bouhafs, H. Aourag, M. Certier, *J. Phys., Condens. Matter* 10 (1998) 4975.  
 [26] D. Gerlich, S.L. Dole and G.A. Slack, *J. Phys. Chem. Solids* 47 (1986) 437.  
 [27] J. Petalas, S. Logothetidis, S. Boultaidakis, *Phys. Rev. B* 52 (1995) 8082.  
 [28] A. Trampert, O. Brandt, K.H. Ploog, *Acad. Press*, 50 1998.  
 [29] S. Berrah, H. Abid, A. Boukortt, M. Sehil, *Turk J Phys.*, 30 (2006) 513-518.  
 [30] S. Q. Wang and H. Q. Ye., *J. Phys., Condens. Matter*, 14 (2002) 9579.  
 [31] Donald T. Morelli, Glen A. Slack, *HTCM*, (2006) 37-68.  
 [32] J. Petalas, S. Logothetidis, S. Boultaidakis, *Phys. Rev. B* 52 (1995) 8082.  
 [33] D. Sedmidubsk, J. Leitner, P. Svoboda, Z. Soferand, J. Macháček, *J. Thermal Analysis and Calorimetry*, 95 2 (2009) 403–407.  
 [34] D. Gerlich, S.L. Dole and G.A. Slack, *J. Phys. Chem. Solids*, 47 (1986) 437.

**Figure 1** Total energy (Ry) variation with lattice parameters in Bohr (a.u) are plotted for zinc-blende cBN and cGaN for obtaining the equilibrium (P=0, T=0) lattice parameters.

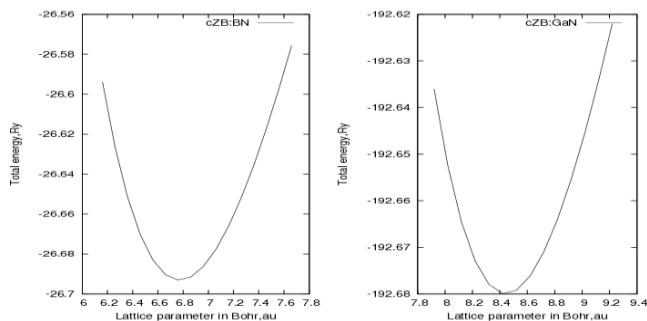


**Figure 2** Volume variation with pressure is calculated and plotted for cBN and cGaN at two extreme temperature T=0K, 1500K.

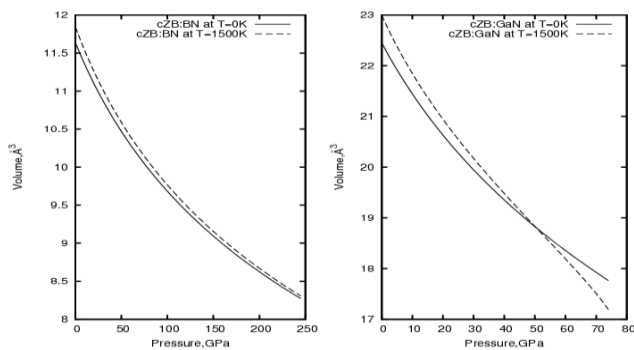


**Figure 3** Volume variation with temperature is calculated and plotted for cBN and cGaN at two extreme pressure  $P=0\text{GPa}$ ,  $150\text{GPa}$  for cBN and  $P=0\text{GPa}$ ,  $50\text{GPa}$  for the cGaN.

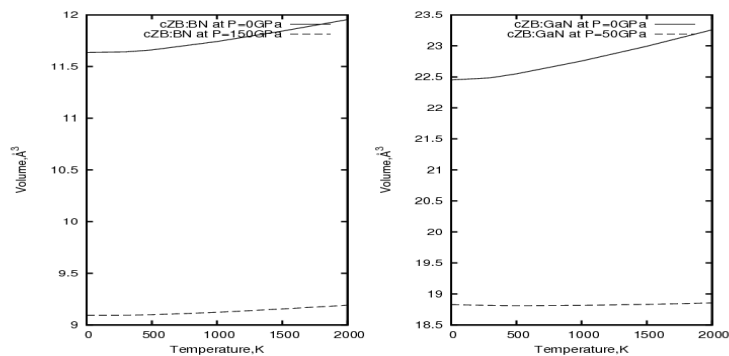


**Figure 4** Debye temperature variations with temperature for cBN and cGaN at equilibrium lattice parameters.

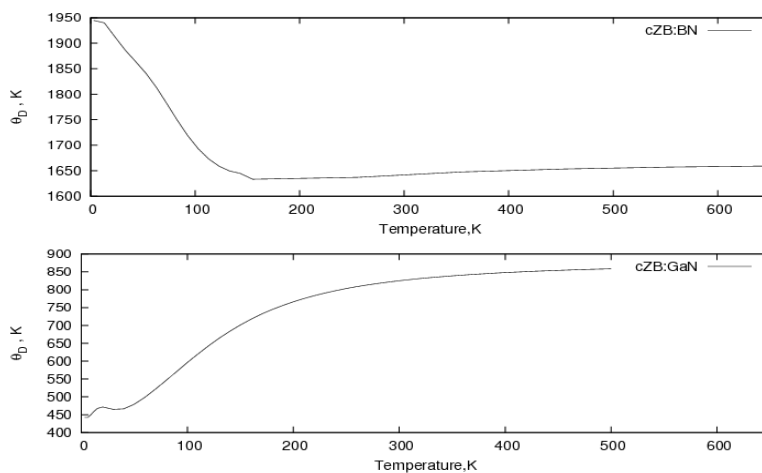


**Figure 5** Total Phonon DOS of cBN with each elemental atom phonon DOS of B and N

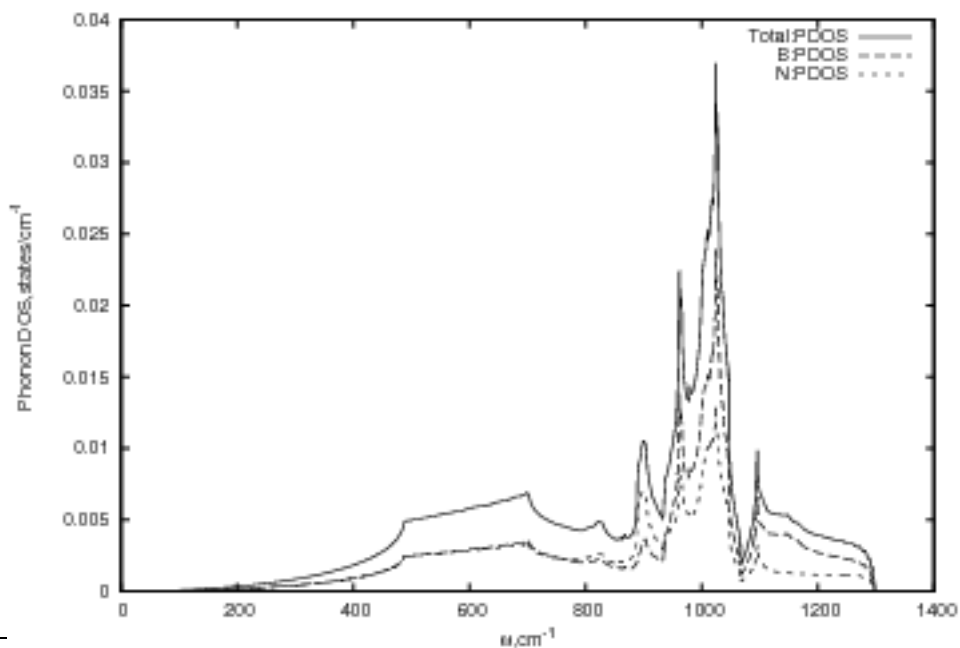


**Figure 6** Total Phonon DOS of cGaN with each elemental atom phonon DOS of Ga and N

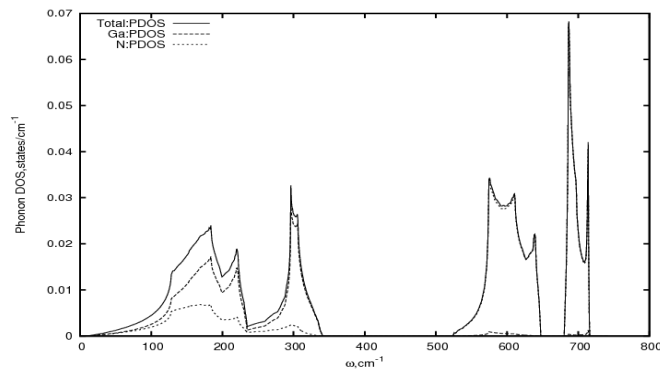


**Figure 7** Heat capacity  $C_p$  at two extreme pressure  $P=0\text{GPa}, 150\text{GPa}$  for cBN and  $P=0\text{GPa}, 50\text{GPa}$  for cGaN are shown.

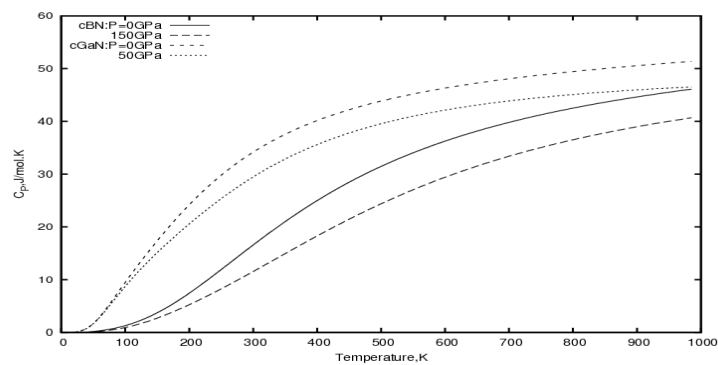


**Figure 8**  $C_p/T^3$  verse T graph at two extreme pressure  $P=0\text{GPa}, 150\text{GPa}$  for cBN and  $P=0\text{GPa}, 50\text{GPa}$  for cGaN are shown.

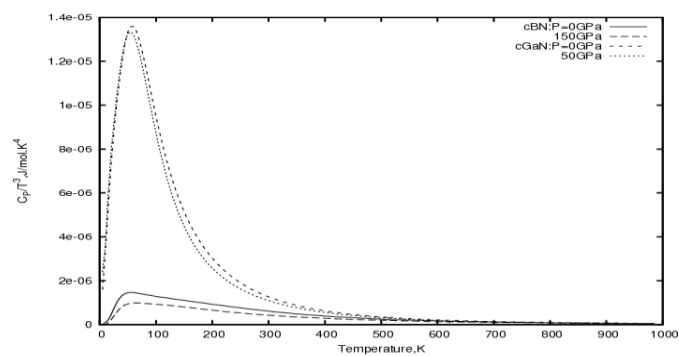


**Table 1** All the calculated properties are tabulated and compare with experimental and results obtained from others workers for cBN and cGaN.

Parameters	Our Work		Others		Experimental	
	cBN	cGaN	cBN	cGaN	cBN	cGaN
$a_0(\text{Å})$	3.582	4.467	3.582 <sup>a</sup>	4.475 <sup>l</sup> , 4.335 <sup>m</sup>	3.615 <sup>e</sup>	4.52 <sup>k</sup>
$B_0(\text{GPa})$	390.45	196.5	391 <sup>a</sup> at 300K	205.38 <sup>l</sup> , 207 <sup>m</sup>	369–465 <sup>c</sup>	190 <sup>k</sup>
$B_0'$	3.77	4.57	3.18 <sup>b</sup> , 3.94 <sup>j</sup>	4.8 <sup>l</sup> , 4.182 <sup>m</sup>		
$V_0(\text{Å}^3/\text{atom})$	5.747	22.279	5.745 <sup>a</sup>		5.905 <sup>e</sup>	
$C_{11}(\text{GPa})$	820.39	287.84	844 <sup>l</sup> , 754 <sup>b</sup>		820 <sup>e</sup>	

*Heat Capacity of BN and GaN binary semiconductor under high Pressure-Temperature (PT) from*

C <sub>12</sub> (GPa)	192.853	158.67	190 <sup>f</sup> , 179 <sup>b</sup>		190 <sup>g</sup>
C <sub>44</sub> (GPa)	475.013	160.07	480 <sup>f</sup> , 433 <sup>b</sup>		480 <sup>g</sup>
B <sub>0</sub> (GPa) (C <sub>ij</sub> )	402.032	201.73	377 <sup>b</sup>		
Poisson's ratio(v)	0.12486	0.26738			
v <sub>R</sub>	0.13063	0.28621			
v <sub>V</sub>	0.11909	0.24855			
Θ <sub>D</sub> (K)	1530.46	496.38		390 <sup>n</sup>	
Θ <sub>D</sub> (K) QHA	1665.33	833.09	1710 <sup>b</sup>	823 <sup>p</sup> , 600- 800 <sup>o</sup> , 867 <sup>q</sup>	1700 <sup>h</sup>

<sup>a</sup>Reference[1]

<sup>d</sup>Reference[19]

<sup>g</sup>Reference[22]

<sup>j</sup>Reference[25]

<sup>m</sup>Reference[30]

<sup>p</sup>Reference[33]

<sup>b</sup>Reference[17]

<sup>e</sup>Reference[20]

<sup>h</sup>Reference[23]

<sup>k</sup>Reference[28]

<sup>n</sup>Reference[31]

<sup>q</sup>Reference[34]

<sup>c</sup>Reference[18]

<sup>f</sup>Reference[21]

<sup>i</sup>Reference[24]

<sup>l</sup>Reference[29]

<sup>o</sup>Reference[32]